Brain-Computer Interface Controlled Robotic Gait Orthosis: A Case Report

An H. Do[1,2], Po T. Wang[3], Christine E. King[3], Sophia N. Chun[4], Zoran Nenadic[3,5]

***Abstract*—An able-bodied subject used walking motor imagery to accurately operate a non-invasive brain-computer interface (BCI) controlled robotic gait orthosis. This finding represents the first successful demonstration of a BCI-controlled lower extremity prosthesis for independent ambulation, with significant implications for restoring ambulation to individuals with spinal cord injury paraplegia.**

***Index Terms*—Brain computer interface, gait, walking, robotic gait orthosis, Lokomat.**

I. Introduction

INDIVIDUALS with paraplegia due to spinal cord injury (SCI) are unable to walk and most are wheelchair bound. In addition, decreased physical activity results in a wide range of comorbidities such as metabolic derangements, heart disease, osteoporosis, and pressure ulcers [1]. Treatment of these conditions contributes to the bulk of medical care costs for this patient population [1]. While wheelchairs and lower extremity prostheses assist with mobility after SCI, no biomedical solutions can reverse this loss of neurological function. Hence, novel approaches are being pursued to restore able-bodied-like ambulation in patients with SCI. If successful, these will improve the quality of life in this population, and reduce the incidence and cost of medical comorbidities and care-giver burden.

A non-invasive brain-computer interface (BCI) controlled lower extremity prosthesis may be the first step towards developing a biomechanical means to restore able-bodied-like ambulation after SCI. Such a system could enable SCI patients to use their electroencephalogram (EEG) to control the walking function of a lower extremity prosthesis. However, the integration of a BCI and a lower extremity prosthesis has not yet been realized. The feasibility of BCI-controlled ambulation was explored in the authors' prior work [2], [3], in which subjects (both able-bodied and SCI) used an EEG-based BCI to control the ambulation of an avatar within a virtual reality environment. Pursuant to these findings, the authors report on the first integration of an EEG-based BCI with a robotic gait orthosis (RoGO), and its successful operation by a single able-bodied subject.

[1]Division of Neurology, Long Beach Veterans Affairs Medical Center (LBVA), Long Beach, CA, USA
[2]Department of Neurology, University of California, Irvine (UCI), CA, USA, email: and@uci.edu
[3]Department of Biomedical Engineering, UCI, CA, USA
[4]Department of Spinal Cord Injury, LBVA, Long Beach, CA, USA
[5]Department of Electrical Engineering and Computer Science, UCI, CA, USA

II. Methods

To facilitate the development of a BCI-controlled RoGO, EEG data were recorded from an able-bodied subject engaged in alternating epochs of walking and standing motor imagery (MI). These data were analyzed to generate an EEG prediction model for online BCI operation. A commercial RoGO system (suspended over a treadmill), was interfaced with the BCI computer to allow for computerized control. In an online test, the subject was tasked to ambulate using the BCI-RoGO system when prompted by computerized cues. The performance of this system was assessed with cross-correlation analysis, latency, and omission and false alarm rates.

A. Training Data Acquisition

Ethical approval was obtained from the Institutional Review Board at the LBVA and UCI. An able-bodied male subject (age 42, with $\sim$5 hr of BCI experience) gave informed consent to participate in the study. First, an actively shielded 64-channel EEG cap was mounted on the subject's head with impedances reduced to $<$10 KΩ. EEG signals were acquired using 2 linked NeXus-32 bioamplifiers (Mind Media, Roermond-Herten, The Netherlands) at a sampling rate of 256 Hz. The subject was then suspended into a treadmill-equipped RoGO (Lokomat, Hocoma, Volketswil, Switzerland) using partial weight unloading (see Fig. 1). Note that unlike overground orthoses, this system facilitates safe and easy testing suitable for early development of BCI-prostheses for ambulation. Finally, EEG data were collected as the subject alternated between 30-sec epochs of standing and walking MI for a total of 10 min, as directed by the computer cues. The subject was instructed to stand still with arms at the sides.

B. Electromyogram and Leg Movement Measurement

Electromyogram (EMG) was measured to rule out BCI control by voluntary leg movements. To this end, baseline lower extremity EMG were measured under 3 conditions: *active walking* (subject voluntarily walks while the RoGO servos are turned off); *cooperative walking* (subject walks synergistically with the RoGO); and *passive walking* (the subject is fully relaxed while the RoGO makes walking movements). Three pairs of surface EMG electrodes were placed over the left quadriceps, tibialis anterior, and gastrocnemius (Fig. 1), and signals were acquired with a bioamplifier (MP150, Biopac, Goleta, CA), bandpass filtered (0.1-1000 Hz), and sampled at 4 KHz. In addition, a gyroscope (Wii Motion Plus, Nintendo, Kyoto, Japan) with a custom wristwatch-like enclosure was

strapped to the distal left lower leg (proximal to the ankle), and was used to measure leg movements (Fig. 1) [4]. Approximately 85% body-weight unloading was necessary for proper RoGO operation, and the walking velocity was set at 2 km/hr.

C. Offline Analysis

An EEG prediction model was generated using the methods described in [5], which are briefly summarized here. First, the training EEG data were subjected to an automated algorithm to exclude EEG channels with excessive artifacts. The EEG epochs corresponding to "idling" and "walking" states were transformed into the frequency domain, and their power spectral densities (PSD) were integrated over 2-Hz bins. The data then underwent dimensionality reduction using a combination of classwise principal component analysis (CPCA) [6], [7] and approximate information discriminant analysis (AIDA) [8]. The resulting 1-D spatio-spectral features were extracted by:

$$f = T_A \Phi_C(d) \tag{1}$$

where $f \in \mathbb{R}$ is the feature, $d \in \mathbb{R}^{B \times C}$ are single-trial spatio-spectral EEG data (B-the number of frequency bins, C-the number of retained EEG channels), $\Phi_C : \mathbb{R}^{B \times C} \rightarrow \mathbb{R}^m$ is a piecewise linear mapping from the data space to the m-dimensional CPCA-subspace, and $T_A : \mathbb{R}^m \rightarrow \mathbb{R}$ is an AIDA transformation matrix. Detailed descriptions of these techniques are found in [7], [8]. A linear Bayesian classifier:

$$f^\star \in \begin{cases} \mathcal{I}, & \text{if} \quad P(\mathcal{I}\,|f^\star) > P(\mathcal{W}\,|f^\star) \\ \mathcal{W}, & \text{otherwise} \end{cases} \tag{2}$$

was then designed in the feature domain, where $P(\mathcal{I}\,|f^\star)$ and $P(\mathcal{W}\,|f^\star)$ are the posterior probabilities of "idling" and "walking" classes, respectively. The performance of the Bayesian classifier (2), expressed as a classification accuracy, was then assessed by performing stratified 10-fold cross-validation [9]. This was achieved by using 90% of the EEG data to train the parameters of the CPCA-AIDA transformation and the classifier. The remaining 10% of data then underwent the above transformation and classification. This process was repeated 10 times, each time using a different set of 9 folds for training and the remaining 1 fold for testing. Finally, the optimal frequency range $[F_L, F_H]$ was found by increasing the lower and upper frequency bounds and repeating the above procedure until the classifier performance stopped improving [5]. The parameters of the prediction model, including $[F_L, F_H]$, the CPCA-AIDA transformation, and the classifier parameters, were then saved for future real-time EEG analysis during online BCI-RoGO operation. The above signal processing and pattern recognition algorithms were implemented into the BCI software and optimized for real-time operation [5].

D. BCI-RoGO Integration

To comply with the institutional restrictions that prohibit software installation, the RoGO computer was interfaced with the BCI using a pair of microcontrollers to perform mouse hardware emulation. Microcontroller #1 relayed commands from the BCI computer to microcontroller #2 via an Inter-Integrated Circuit (I^2C) connection. Microcontroller #2 then acted as a slave device programmed with a mouse emulation firmware [10] to automatically manipulate the RoGO's user interface. This setup enabled the BCI computer to directly control the RoGO idling and walking functions.

E. Online Signal Analysis

During online BCI-RoGO operation, blocks of EEG data were acquired every 0.25 sec. The PSD of the retained EEG channels were calculated and used as the input for the signal processing algorithms (Section II-C).

F. Calibration

Similar to the authors' prior work [2], [3], [5], [11], [12], the BCI-RoGO system is modeled as a binary state machine with "idling" and "walking" states. The posterior probability averaged over 2 sec of EEG data, $\bar{P}(W|f^\star)$, was compared to two thresholds, T_I and T_W, to initiate state transitions. Specifically, the system transitioned from "idling" to "walking" state (and vice versa) when $\bar{P} > T_W$ ($\bar{P} < T_I$), respectively. Otherwise, the system remained in the current state.

This calibration procedure was used to determine the values of T_I and T_W. The system was set to run in the online mode (but without the RoGO walking) as the subject alternated between idling or walking MI for $\sim$5 min. The values of $\bar{P}$ were plotted in a histogram to help empirically determine the values of T_I and T_W. A brief familiarization online session with feedback further fine-tuned these threshold values. The delay of processing a 2-sec EEG segment was $\sim$0.125 sec.

G. Online Evaluation

In an online evaluation, the subject, while mounted in the RoGO, used idling/walking MI to elicit 5 alternating 1-min epochs of BCI-RoGO idling/walking, as directed by the computer cues. Ideally, during walking MI, the underlying EEG changes should initiate and maintain BCI-RoGO walking until walking MI stops. The subject was instructed to make no voluntary movements and to keep arms still at the side. Left leg EMG and movements were measured as described in Section II-B. This evaluation task was performed 5 times.

Online performance was assessed with the following metrics [5], [11], [12]: 1. Cross-correlation between the cues and BCI-RoGO walking, 2. Omissions (OM)—failure to activate BCI-RoGO walking during "Walk" cues, and 3. False Alarms (FA)—initiation of BCI-RoGO walking during "Idle" cues.

Analysis of EMG and leg movement data was performed to ascertain that RoGO walking was entirely BCI controlled. First, to demonstrate that covert movements were not used to initiate BCI-RoGO walking, gyroscope and rectified EMG data (in the 40-400 Hz band) were compared to the BCI decoded "walking" states in each session. Ideally, the initiation of these states should precede EMG activity and leg movements. Then, to establish that voluntary movements were not used to maintain BCI-RoGO walking, EMG during these epochs were compared to the baselines (see Section II-B). To this end,

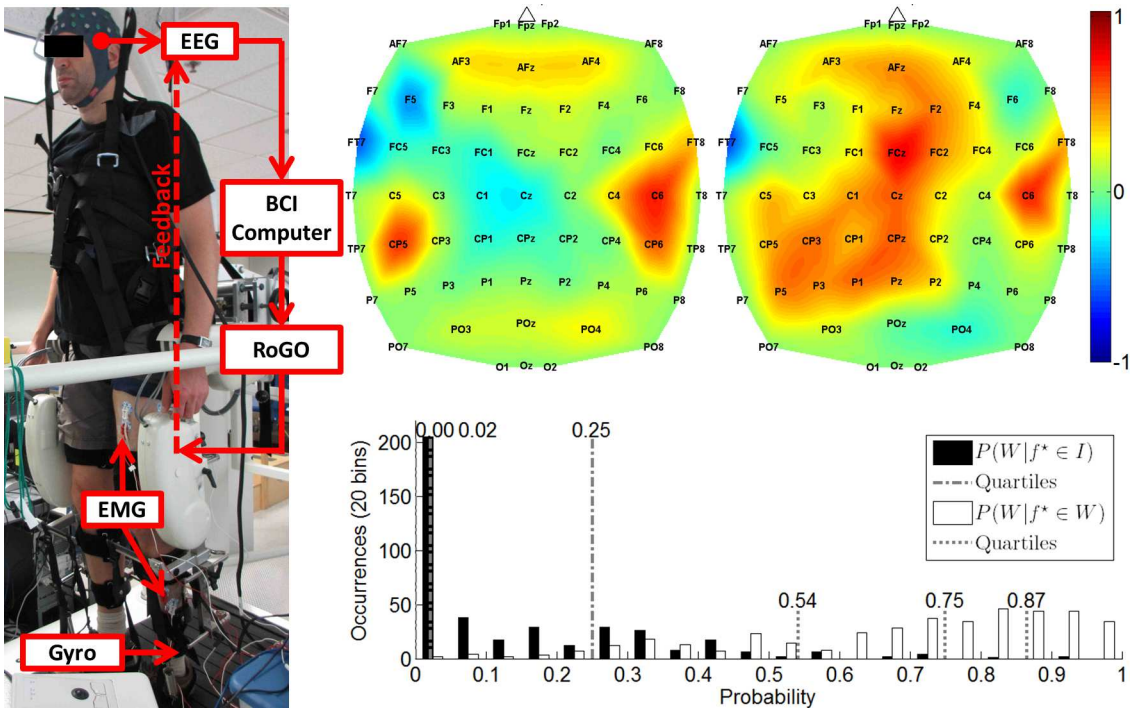

Fig. 1. *Left*: The experimental setup showing the subject suspended in the RoGO, while donning an EEG cap, surface EMG electrodes, and a gyroscope on the left leg. A monitor (not shown), placed in front of the subject at eye-level, presented instructional cues. *Top Right*: The CPCA-AIDA feature extraction maps at the 8-10 Hz bin. Since feature extraction is piecewise linear, there is one map for each of the 2 classes. Brain areas with values close to +1 or -1 are most salient for distinguishing between idling and walking classes at this frequency. *Bottom Right*: Histogram of averaged posterior probabilities, $\bar{P}(W|f^\star)$.

EMG data were segmented by individual steps based on the leg movement pattern [4]. The PSD of these EMG segments were then averaged and compared to those of the baseline walking conditions. Ideally, the EMG power during BCI-RoGO walking should be similar to that of *passive walking* and should differ from those of *active* and *cooperative walking*.

III. Results

An EEG prediction model was generated as described in Section II-C based on training EEG data (Section II-A). This offline analysis resulted in a model classification accuracy of 94.8±0.8% (chance: 50%). A representative EEG feature extraction map is shown in Fig. 1. After the calibration procedure (Section II-F), a histogram of posterior probabilities was plotted (Fig. 1). Based on this and a familiarization trial, the values $T_I = 0.04$ and $T_W = 0.65$ were ultimately chosen.

The performances from the 5 online sessions are summarized in Table I. The average cross-correlation between instructional cues and the subject's BCI-RoGO walking epochs was 0.809 ± 0.056. For control, the maximum cross-correlation between instructional cues and simulated BCI operation using 100,000 Monte Carlo random walk runs was 0.408, indicating that the cross-correlations in Table I were significant with an empirical p-value$<10^{-5}$. Also, there were no omissions. However, in the first 3 sessions, one to two brief false alarms occurred, and there were none during the final 2 sessions. False alarm epochs averaged 7.08 sec, but much of this time can be attributed to the RoGO's locked-in startup sequence ($\sim$5 sec). A supplemental video of a representative session is provided at http://www.youtube.com/watch?v=W97Z8fEAQ7g.

TABLE I
ONLINE PERFORMANCES: CROSS-CORRELATION BETWEEN BCI-ROGO WALKING AND CUES AT SPECIFIC LAGS, NUMBER OF OMISSIONS AND FALSE ALARMS, AND AVERAGE DURATION OF FALSE ALARM EPOCHS.

Sess.	Xcorr. (lag in sec)	OM	FA (avg. duration in sec)
1	0.771 (10.25)	0	1 (12.0)
2	0.741 (4.50)	0	2 (5.5±0.0)
3	0.804 (3.50)	0	1 (5.3)
4	0.861 (4.50)	0	0
5	0.870 (12.00)	0	0
Avg.	0.809±0.056 (6.95±3.89)	0	0.8 (7.08±3.28)

The EMG and leg movement data from online sessions were analyzed as described in Section II-G. EMG and gyroscope measurements indicated that no movement occurred prior to the initiation of BCI decoded "walking" states (see Fig. 2). When compared to the baselines, the EMG during online BCI-RoGO walking in all 3 muscle groups were statistically different from those of *active* or *cooperative walking* conditions ($p<10^{-13}$), and were not different from those of passive walking ($p=0.37$). These results confirm that the BCI-RoGO system was wholly BCI controlled. Note that *passive walking* is known to generate EMG activity [13], hence a similar level of activity during BCI-RoGO walking (Fig. 2) is expected.

IV. Discussion and Conclusion

Despite standing while suspended in the RoGO, the EEG prediction model's classification accuracy was higher than those from the same training procedure when performed in the seated condition [2], [3]. Also, the salient brain areas underlying walking MI (Fig. 1) were consistent with those

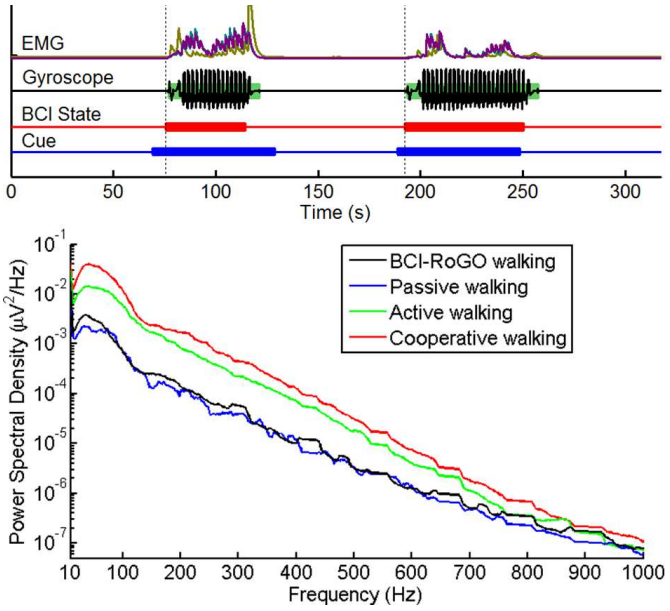

Fig. 2. *Top*: Results from a representative online session, showing epochs of idling and BCI-RoGO walking (red trace: decoded BCI states; blue trace: instructional cues). The thick/thin blocks indicate walking/idling. Corresponding EMG (gold: quadriceps; teal: tibialis anterior; purple: gastrocnemius) and BCI-RoGO walking as detected by the gyroscope are also shown. *Bottom*: Representative EMG PSD of the quadriceps, demonstrating that EMG during BCI-RoGO walking are different from baseline active or cooperative walking conditions, and are similar to passive walking.

previously reported. These areas likely overlie the pre-frontal cortex, supplementary motor (SMA), and arm motor representation areas. Activation of the pre-frontal cortex and SMA during walking MI has been described in functional imaging studies (e.g. [14]). Involvement of bilateral arm areas during walking MI may be associated with arm swing imagery [3]. Finally, this EEG prediction model was further validated by generating separable posterior probability distributions (Fig. 1) and facilitating highly accurate online BCI-RoGO control.

The average online cross-correlation (Table I) was higher than those achieved with upper (0.78) and lower (0.67) extremity BCI-prostheses [11], [5], despite EEG being acquired under more hostile (ambulatory) conditions. This implies that future BCI-prostheses for overground walking may be feasible. Additionally, the subject's online BCI-RoGO operation was purposeful with a 100% response rate (no omissions), and by the end of the experiment, the subject had no false alarms. Although brief in duration, false alarms carry the risk of bodily harm in future BCI-prostheses for overground walking. These could be minimized using a longer posterior probability window and longer practice in a controlled environment.

With only $\sim$5 hr of BCI experience (operating the BCI walking avatar in [2], [3]), the subject attained a high-level of control of the BCI-RoGO system after a very short procedure (10 min training data acquisition, 5 min calibration, 5 min familiarization). This indicates that a data-driven EEG prediction model as well as prior virtual reality training may have facilitated this rapid acquisition of control. In addition, the BCI operation was achieved using an intuitive control strategy, i.e. walking MI to induce walking and idling MI to stand.

In conclusion, these results provide preliminary evidence that restoring brain-controlled ambulation may be possible. However, future work is necessary to test this system in individuals with paraplegia due to SCI. Since SCI users are able to operate the BCI-walking simulator [3], it is expected that they can readily transfer their skills to the BCI-RoGO system like the able-bodied subject here. If successful, such a system can be applied to incomplete motor SCI, where it could add Hebbian learning to gait rehabilitation to improve neurological outcomes beyond those of standard physiotherapy. Finally, it may justify future development of BCI-controlled lower extremity prostheses for free overground walking for those with complete paraplegia due to SCI. This includes addressing issues such as additional degrees of freedom (e.g. turning, velocity, sitting, standing), as well as appropriate solutions for signal acquisition (e.g. invasive recordings).

Acknowledgment

This project was funded by the Long Beach Veterans Affairs Southern California Institute for Research and Education (SCIRE) Small Projects Grant, and the Long Beach Veterans Affairs Advanced Research Fellowship Grant.

References

[1] R. L. Johnson, C. A. Brooks, and G. G. Whiteneck, "Cost of traumatic spinal cord injury in a population-based registry." *Spinal Cord*, vol. 34, no. 8, pp. 470–480, 1996.

[2] P. T. Wang, C. E. King, L. A. Chui, Z. Nenadic, and A. H. Do, "BCI controlled walking simulator for a BCI driven FES device," in *Proc of RESNA Ann Conf*, 2010.

[3] P. T. Wang, C. E. King, L. A. Chui, A. H. Do, and Z. Nenadic, "Self-paced brain-computer interface control of ambulation in a virtual reality environment," *J Neural Eng (under revision)*, 2012.

[4] K. Aminian, B. Najafi, C. Büla, P. F. Leyvraz, and P. Robert, "Spatio-temporal parameters of gait measured by an ambulatory system using miniature gyroscopes." *J Biomech*, vol. 35, no. 5, pp. 689–699, 2002.

[5] A. H. Do, P. T. Wang, A. Abiri, C. E. King, and Z. Nenadic, "Brain-computer interface controlled functional electrical stimulation system for ankle movement." *J Neuroeng Rehabil*, vol. 8, no. 49, 2011.

[6] K. Das, S. Osechinskiy, and Z. Nenadic, "A classwise PCA-based recognition of neural data for brain-computer interfaces," in *Proc IEEE Eng Med Biol Soc*, 2007, pp. 6519–6522.

[7] K. Das and Z. Nenadic, "An efficient discriminant-based solution for small sample size problem," *Pattern Recogn*, vol. 42, no. 5, pp. 857–866, 2009.

[8] ——, "Approximate information discriminant analysis: A computationally simple heteroscedastic feature extraction technique," *Pattern Recogn*, vol. 41, no. 5, pp. 1548–1557, 2008.

[9] R. Kohavi, "A study of cross-validation and bootstrap for accuracy estimation and model selection," in *Int Joint C Art Int*, 1995, pp. 1137–1145.

[10] Darran. (2011, Mar) Arduino UNO Mouse HID version 0.1. Arduino Hacking. [Online]. Available: http://hunt.net.nz/users/darran/

[11] C. E. King, P. T. Wang, M. Mizuta, D. J. Reinkensmeyer, A. H. Do, S. Moromugi, and Z. Nenadic, "Noninvasive brain-computer interface driven hand orthosis," in *Proc 33rd Ann Int Conf of the IEEE Eng in Med and Biol Soc*, 2011, pp. 5786–5789.

[12] A. H. Do, P. T. Wang, C. E. King, A. Schombs, S. C. Cramer, and Z. Nenadic, "Brain-computer interface controlled functional electrical stimulation device for foot drop due to stroke," in *Proc 34th Ann Int Conf of the IEEE Eng in Med and Biol Soc (accepted)*, 2012.

[13] S. Mazzoleni, G. Stampacchia, E. Cattin, E. Bradaschia, M. Tolaini, B. Rossi, and M. C. Carrozza, "Effects of a robot-mediated locomotor training on EMG activation in healthy and SCI subjects," in *Proc IEEE Int Conf Rehab Robotics*, 2009, pp. 378–382.

[14] C. La Fougère, A. Zwergal, A. Rominger, S. Förster, G. Fesl, M. Dieterich, T. Brandt, M. Strupp, P. Bartenstein, and K. Jahn, "Real versus imagined locomotion: a [18F]-FDG PET-fMRI comparison." *Neuroimage*, vol. 50, no. 4, pp. 1589–1598, 2010.